

The Polyphosphate Kinase of Escherichia coli Is Required for Full Production of the Genotoxin Colibactin

Min Tang-Fichaux, Camille Chagneau, Nadège Bossuet-Greif, Jean-Philippe Nougayrède, Eric Oswald, Priscilla Branchu

▶ **To cite this version:**

Min Tang-Fichaux, Camille Chagneau, Nadège Bossuet-Greif, Jean-Philippe Nougayrède, Eric Oswald, et al.. The Polyphosphate Kinase of Escherichia coli Is Required for Full Production of the Genotoxin Colibactin. MSphere, 2020, 5 (6), pp.1-14. 10.1128/mSphere.01195-20 . hal-03134525

HAL Id: hal-03134525
https://hal.inrae.fr/hal-03134525

Submitted on 8 Feb 2021

HAL is a multi-disciplinary open access archive for the deposit and dissemination of scientific research documents, whether they are published or not. The documents may come from teaching and research institutions in France or abroad, or from public or private research centers.

L'archive ouverte pluridisciplinaire **HAL**, est destinée au dépôt et à la diffusion de documents scientifiques de niveau recherche, publiés ou non, émanant des établissements d'enseignement et de recherche français ou étrangers, des laboratoires publics ou privés.



Distributed under a Creative Commons Attribution 4.0 International License

AMERICAN SOCIETY FOR MICROBIOLOGY | mSphere®

RESEARCH ARTICLE
Molecular Biology and Physiology

The Polyphosphate Kinase of *Escherichia coli* Is Required for Full Production of the Genotoxin Colibactin

Min Tang-Fichaux,[a] Camille V. Chagneau,[a] Nadège Bossuet-Greif,[a] Jean-Philippe Nougayrède,[a] Éric Oswald,[a,b] Priscilla Branchu[a]

[a]IRSD, Université de Toulouse, INSERM, INRAE, ENVT, UPS, Toulouse, France
[b]CHU Toulouse, Service de Bactériologie-Hygiène, Toulouse, France

Éric Oswald and Priscilla Branchu jointly supervised this work and are co-senior authors.

ABSTRACT Colibactin induces DNA damage in mammalian cells and has been linked to the virulence of *Escherichia coli* and the promotion of colorectal cancer (CRC). By looking for mutants attenuated in the promoter activity of *clbB* encoding one of the key enzymes for the production of colibactin, we found that a mutant of the gene coding for the polyphosphate kinase (PPK) produced less colibactin than the parental strain. We observed this phenotype in different strains ranging from pathogens responsible for meningitis, urinary tract infection, or mouse colon carcinogenesis to the probiotic Nissle 1917. We confirmed the role of PPK by using an inhibitor of PPK enzymatic activity, mesalamine (also known as 5-aminosalicylic acid). Interestingly, mesalamine has a local anti-inflammatory effect on the epithelial cells of the colon and is used to treat inflammatory bowel disease (IBD). Upon treatment with mesalamine, a decreased genotoxicity of colibactin-producing *E. coli* was observed both on epithelial cells and directly on purified DNA. This demonstrates the direct effect of mesalamine on bacteria independently from its anti-inflammatory effect on eukaryotic cells. Our results suggest that the mechanisms of action of mesalamine in treating IBD and preventing CRC could also lie in the inhibition of colibactin production. All in all, we demonstrate that PPK is required for the promoter activity of *clbB* and the production of colibactin, which suggests that PPK is a promising target for the development of anticolibactin and antivirulence strategies.

IMPORTANCE Colibactin-producing *E. coli* induces DNA damage in eukaryotic cells and promotes tumor formation in mouse models of intestinal inflammation. Recent studies have provided strong evidence supporting the causative role of colibactin in human colorectal cancer (CRC) progression. Therefore, it is important to understand the regulation of the production of this genotoxin. Here, we demonstrate that polyphosphate kinase (PPK) is required for the promoter activity of *clbB* and the production of colibactin. Interestingly, PPK is a multifunctional player in bacterial virulence and stress responses and has been proposed as a new target for developing antimicrobial medicine. We observed inhibition of colibactin production by using a previously identified PPK inhibitor (i.e., mesalamine, an anti-inflammatory drug commonly prescribed for inflammatory bowel diseases). These data brought us a new perspective on the regulatory network of colibactin production and provided us a clue for the development of anticolibactin strategies for CRC treatment/prophylaxis.

KEYWORDS *pks*, genotoxicity, PPK, mesalamine, colibactin

Colibactin is a natural genotoxic compound produced primarily by *Escherichia coli* carrying the 54-kb *pks* genomic island (1). The *pks* island, harboring 19 genes (*clbA* to *clbS*), encodes enzymes responsible for the synthesis of colibactin. Nonribosomal

Citation Tang-Fichaux M, Chagneau CV, Bossuet-Greif N, Nougayrède J-P, Oswald É, Branchu P. 2020. The polyphosphate kinase of *Escherichia coli* is required for full production of the genotoxin colibactin. mSphere 5:e01195-20. https://doi.org/10.1128/mSphere.01195-20.

Editor Sarah E. F. D'Orazio, University of Kentucky

Copyright © 2020 Tang-Fichaux et al. This is an open-access article distributed under the terms of the Creative Commons Attribution 4.0 International license.

Address correspondence to Éric Oswald, eric.oswald@inserm.fr, or Priscilla Branchu, priscilla.branchu@inrae.fr.

Received 23 November 2020
Accepted 24 November 2020
Published 16 December 2020

peptide synthases (NRPSs; i.e., ClbN, ClbH, and ClbJ), polyketide synthases (PKSs; i.e., ClbC, ClbI, and ClbO), and hybrid NRPS-PKSs (i.e., ClbB and ClbK) constitute an assembly line which is activated by phosphopantetheinyl transferase ClbA (2). Following activation by ClbA, the initiating NRPS ClbN uses asparagine as a substrate to generate the prodrug motif *N*-myristoyl-D-Asn (C_{14}AsnOH) (3). Then, ClbB accepts C_{14}AsnOH and constructs the amide bond cleavable by the periplasmic membrane-bound peptidase ClbP (3). With continuous actions of other enzymes on the assembly line, precolibactin is synthesized in the cytoplasm and then exported to the periplasm, where precolibactin is cleaved by ClbP to release active colibactin and the prodrug motif C_{14}AsnOH (3).

The warheads of colibactin alkylate DNA on two adenine residues of opposite strands of DNA, which induces a DNA interstrand cross-link (ICL) and ultimately a DNA double-strand break (DSB) (4, 5). These types of DNA damage in eukaryotic cells activate DNA repair pathways, resulting in histone H2AX phosphorylation (producing γH2AX) and senescence (1, 4, 6). Colibactin has been linked to bacterial virulence (7, 8) and microbial diversity (9). *In vivo*, colibactin-producing *E. coli* has been shown to cause DNA damage (10, 11) and tumor formation (12–15) in mouse models of intestinal inflammation. Importantly, a high abundance of colibactin-producing *E. coli* has been found in inflammatory bowel disease (IBD) and colorectal cancer (CRC) patients (12, 15, 16). Furthermore, recent studies have revealed colibactin DNA damage signatures that directly indicate the mutational impact in CRC (4, 6).

Given the role of colibactin in bacterial virulence and tumorigenesis, it is important to understand the regulation of its production, to provide clues for the development of anticolibactin strategies. It was recently reported that ClbR is an (auto)transcriptional activator of the *clbB* gene (17). In addition, the two master regulators of bacterial iron homeostasis Fur (ferric uptake regulator) and the small regulatory noncoding RNA RyhB regulate the transcription of *clbA* (18, 19). *In vivo* studies showed that the expression of *pks* genes was upregulated in human urine (20) and enriched in intestinal inflammation and CRC development (21–23).

In this work, we used a random mutagenesis strategy to find regulators involved in colibactin production. We determined that a mutant of the gene *ppk* encoding polyphosphate kinase (PPK) has a lower *clbB* promoter (P*clbB*) activity than the wild type (WT). PPK catalyzes the reversible conversion of the terminal (γ) phosphate of ATP to long chains of inorganic polyphosphate (polyP; ca. 750 residues), which has been found to be involved in bacterial virulence and stress responses (24). In this work, we found that PPK played a positive role for P*clbB* activity and colibactin production. As mesalamine (also known as 5-aminosalicylic acid) is an inhibitor of PPK enzymatic activity (25), we tested and confirmed that this commonly prescribed drug is capable of inhibiting P*clbB* activity and colibactin biosynthesis.

RESULTS

Identification of PPK as an enhancer of P*clbB* activity. On the assembly line of colibactin, ClbB is the enzyme that accepts the prodrug motif C_{14}AsnOH and constructs the amide bond cleavable by ClbP for releasing active colibactin (3). In order to investigate the regulation of colibactin production, we constructed a transcriptional fusion expressing *luxCDABE* (*lux*) under the control of P*clbB*, resulting in plasmid pMT3a (Table 1; see also Fig. S1a in the supplemental material). This plasmid was transformed into *E. coli* strain SP15, isolated from a patient with neonatal meningitis. Thus, the expression level of luminescence of SP15(pMT3a) reflects P*clbB* activity. Relative luminescence units (RLUs) and optical density at 600 nm (OD_{600}) of SP15(pMT3a) were monitored for 8 h in Dulbecco's modified Eagle's medium (DMEM)-HEPES at 37°C (Fig. 1a). According to RLUs normalized to OD_{600} (RLU/OD_{600}), the peak of P*clbB* activity was just after 4 h. Therefore, we decided to set the measurement time point at 4 h for the following experiments. First, we tested the intrinsic luminescence variability of the WT strain SP15(pMT3a) by measuring RLU/OD_{600} for 300 isolates (Fig. 1b). Relative to (versus) the median value of RLU/OD_{600} of the 300 isolates, the values of RLU/OD_{600} of

TABLE 1 *E. coli* strains and plasmids used in this study

Strain or plasmid	Genotype and/or characteristics[a]	Reference(s) or source
SP15	SP15 with mutation in *rpsL* (Str^r), a derivative of SP15 isolated from spinal fluid of a neonate with meningitis; O18:K1 serotype; colibactin producer	2
Nissle 1917 (EcN)	EcN with mutation in *rpsL* (Str^r), a derivative of the probiotic strain EcN; colibactin producer	35
UTI89	Archetypal uropathogenic *E. coli* isolated from a patient with cystitis; colibactin producer	64
NC101	Commensal murine adherent-invasive *E. coli*; colibactin producer; procarcinogenic in different CRC mouse models	15
SP15 Δ*clbA*	*clbA* mutant of strain SP15; Str^r Kan^r	2
SP15 Δ*clbN*	*clbN* mutant of strain SP15; Str^r Kan^r	2
SP15 Δ*ppk*	*ppk* mutant of strain SP15; Str^r Chl^r	This study
EcN Δ*ppk*	*ppk* mutant of strain EcN; Str^r Chl^r	This study
UTI89 Δ*ppk*	*ppk* mutant of strain UTI89; Chl^r	This study
NC101 Δ*ppk*	*ppk* mutant of strain NC101; Chl^r	This study
SP15(pMT3a)	SP15 containing pMT3a; Str^r Carb^r	This study
P1D10	SP15(pMT3a) with transposon inserted into gene *ppk*; Str^r Carb^r Kan^r	This study
SP15(pMT3)	SP15 containing pMT3; Str^r Kan^r	This study
SP15 Δ*ppk*-c	SP15Δ*ppk* containing pGEN-*ppk*; Str^r Chl^r Carb^r	This study
EcN *clbB*::*lux*	EcN harboring the *clbB* promoter reporter (*luxCDABE*) fusion on the chromosome; Kan^r	17, 26
EcN *clbB*::*lux* Δ*ppk*	EcN *clbB*::*lux* with gene *ppk* disrupted; Kan^r Chl^r	This study
TOP10	Used as host for recombinant plasmids	Thermo Fisher
pCM17	Luciferase-encoding pCM17 vector containing the *ompC* promoter upstream of the *luxCDABE* operon	65
pMT3	*clbB* promoter reporter fusion; Kan^r	This study
pMT3a	*clbB* promoter reporter fusion; Carb^r	This study
pGEN-MCS	Vector of gene *ppk* for complementation of Δ*ppk*; Carb^r	Gift from Ganwu Li
pGEN-*ppk*	pGEN-MCS bearing *ppk* sequence; Carb^r	This study

[a]Str^r, streptomycin resistance; Kan^r, kanamycin resistance; Chl^r, chloramphenicol resistance; Carb^r, carbenicillin resistance.

individual isolates were increased between −20% and +30%; And, relative to the median value of OD_{600}, the OD_{600}s of individual isolates were found to be between −20% and +30%.

Next, a transposon (Tn) mutant library of SP15(pMT3a) was constructed by using the EZ-Tn5 <KAN-2>Tnp Transposome. Under the same condition as described above, RLU/OD_{600} values of 823 Tn mutants were measured at 4 h. Seventeen mutants showing growth retardation compared with the WT (increase of OD_{600} of less than −20%) were excluded; 41 mutants showed an increase of RLU/OD_{600} of less than −20% (Fig. 1c). By sequencing, 40 mutants were identified to have the Tn inserted into the *lux* operon, and 1 mutant (named P1D10) was identified to have the Tn inserted into the gene *ppk* (1,754 bp after the start codon) (Fig. S2). The attenuated P*clbB* activity in P1D10 was also observed by time course monitoring (Fig. 1d).

To confirm that the attenuated P*clbB* activity was due to the inactivation of *ppk* in P1D10, we constructed an isogenic *ppk* deletion mutant of SP15 (SP15 Δ*ppk*). SP15 Δ*ppk* carrying the P*clbB-lux* reporter fusion pMT3 (Table 1) had significantly lower P*clbB* activity than the WT (Fig. 2a and b). Additionally, we deleted *ppk* in the previously described reporter strain Nissle 1917 (EcN) carrying a transcriptional fusion of P*clbB* and the *lux* operon on the chromosome (EcN *clbB*::*lux*) (17, 26), resulting in strain EcN *clbB*::*lux* Δ*ppk* (Fig. S1b). P*clbB* activity was also significantly lower in EcN *clbB*::*lux* Δ*ppk* than in EcN *clbB*::*lux* (Fig. 2c and d). These results consistently suggest that PPK is an enhancer of P*clbB* activity.

PPK is required for full production of colibactin. To determine whether PPK is associated with the biosynthesis of colibactin, we performed DNA interstrand cross-linking (ICL) assays in which bacteria were in direct contact with DNA. The ICL amount is directly correlated with the production of active colibactin (27). After incubation with bacteria, exposed DNA was purified and migrated under the alkaline-denaturing conditions. DNA with ICL is nondenaturable and displays delayed migration compared to that of unaffected denatured single-stranded DNA. Our results showed that SP15 Δ*ppk* caused less ICL than the WT, and this ability was restored in the complemented strain, SP15 Δ*ppk* carrying a plasmid, pGEN-*ppk*, expressing *ppk* (SP15 Δ*ppk*-c) (Fig. 3a

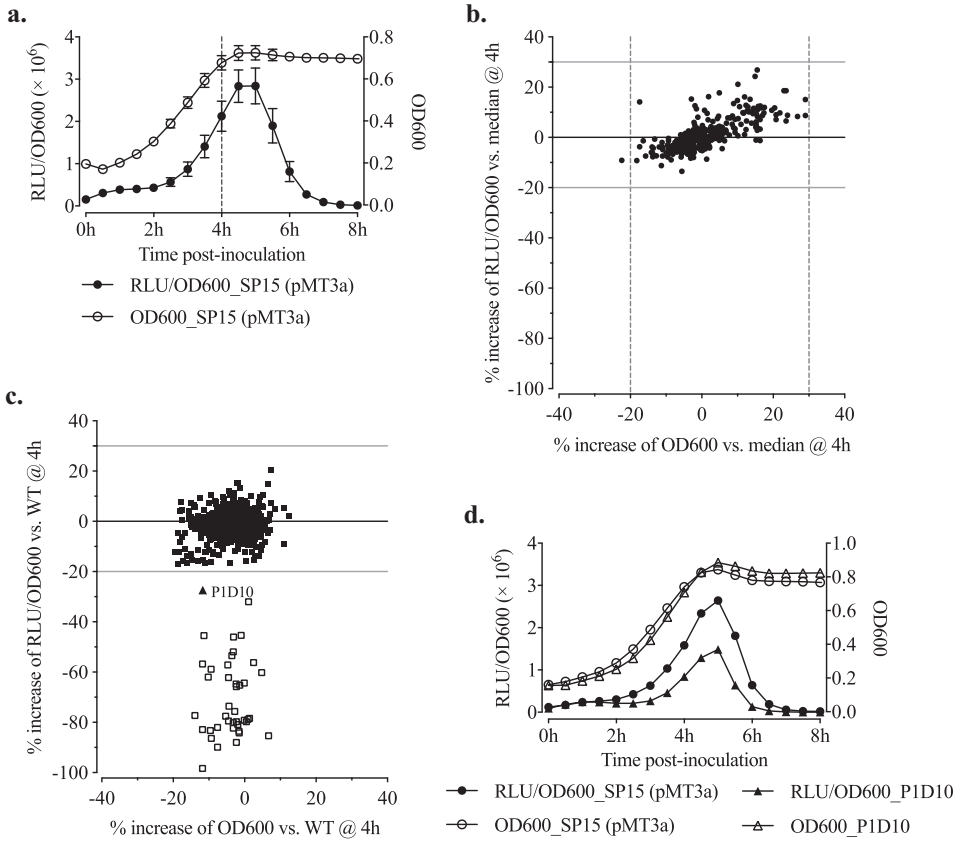


FIG 1 Identification of a mutant of *ppk* having attenuated P*clbB* activity. (a) Time course of P*clbB* activity and growth of SP15(pMT3a) in DMEM-HEPES at 37°C. RLUs were standardized by OD_{600} (RLU/OD_{600}) as the readout for P*clbB* activity. Values are means ± SEMs ($n = 6$ biological replicates). (b) At 4 h, RLU/OD_{600} and OD_{600} of 300 isolates of SP15(pMT3a) were determined. Each black circle represents the increase of RLU/OD_{600} (*y* axis) and OD_{600} (*x* axis) versus the median of 300 isolates. (c) Screening of P*clbB* activities in 806 Tn mutants of SP15(pMT3a) at 4 h in DMEM-HEPES at 37°C. The increase of RLU/OD_{600} or OD_{600} versus the WT are shown. Black squares represent 765 mutants having a variation of increased RLU/OD_{600} or OD_{600} between −20% and 30%. The black triangle represents the mutant P1D10 having −27% increase of RLU/OD_{600} versus WT. White squares represent 40 mutants having less than a −20% increase of RLU/OD_{600} versus that of the WT. (d) Time course P*clbB* activity and growth of P1D10 and the WT [SP15 (pMT3)] in DMEM-HEPES at 37°C. Data are means from two independent experiments.

and b). This *ppk* deletion-associated phenotype was also observed in other strains, including the probiotic strain EcN, the colitogenic strain NC101, and the uropathogenic strain UTI89 (Fig. 3c and d). These results indicate that PPK is required for colibactin biosynthesis in different genetic contexts.

Since colibactin cannot be directly quantified yet, we quantified the production of the prodrug motif C_{14}AsnOH, which is correlated with colibactin production and maturation (Fig. 4a) (3). The result showed that the production level of C_{14}AsnOH of SP15 Δ*ppk* was about 10 times less than that of the WT (Fig. 4b), and this level was restored to the WT level in SP15 Δ*ppk*-c. Taken together, these findings indicate that PPK is required for full P*clbB* activity, thereby enhancing colibactin biosynthesis.

PPK is required for full genotoxicity of colibactin-producing *E. coli*. As ICLs induce the DNA damage response in the host cells, we quantified γH2AX, which is a sensitive marker for colibactin-induced DNA damage by in-cell Western (ICW) assay (2). After a 4-h transient infection and 4 h of growth, HeLa cells grown on a 96-well plate were fixed, and γH2AX was stained by immunofluorescence. The fluorescent signal of γH2AX is pseudocolored in green, and the fluorescent signal of DNA is pseudocolored in red (Fig. 5a). The genotoxic index was determined by quantification of the signal of γH2AX relative to DNA content and normalized to the control (Fig. 5b). The results

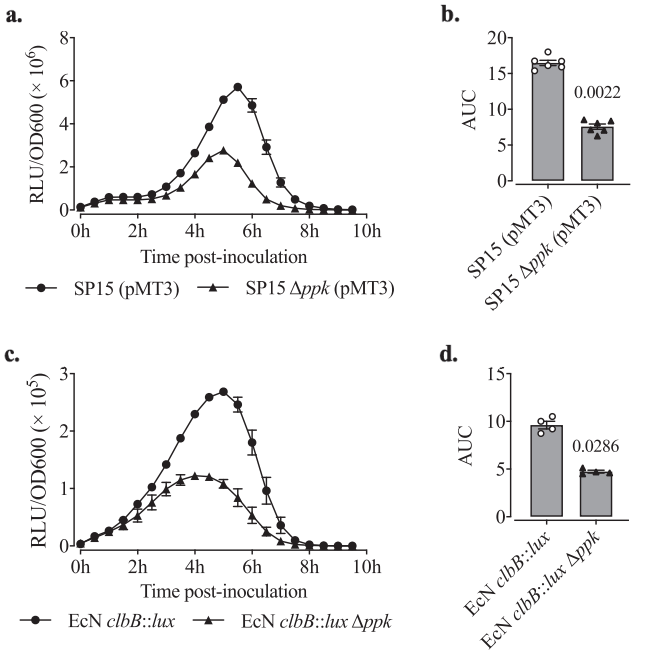


FIG 2 Deletion of *ppk* reduced P*clbB* activity in different genetic contexts using plasmid or chromosomal fusions. (a) Time course RLU/OD_{600} of SP15(pMT3) and SP15 Δ*ppk*(pMT3) grown in DMEM-HEPES at 37°C. (b) Areas under the curves (AUC) of RLU/OD_{600} from panel a. Bars represent means ± SEMs ($n = 6$ biological replicates). The significance was determined using the Mann-Whitney test. P value = 0.0022. (c) Time course RLU/OD_{600} of EcN P*clbB-lux* and EcN P*clbB-lux* Δ*ppk* grown in DMEM-HEPES at 37°C for 10 h. (d) AUC of RLU/OD600 from panel c. Bars represent means ± SEMs ($n = 4$ biological replicates). The significance was determined using the Mann-Whitney test. P value = 0.0286.

showed that the genotoxicity of SP15 Δ*ppk* was significantly lower than that of the SP15 WT and was restored in SP15 Δ*ppk*-c. This indicates that PPK is required for the full genotoxicity of SP15.

Colibactin-producing *E. coli* induces megalocytosis in cultured eukaryotic cells, characterized by a progressive enlargement of the cell body and nucleus and a reduced cell number (1). To corroborate the previous result, we investigated the role of PPK in megalocytosis. Fewer giant cells were observed with infection by SP15 Δ*ppk* than for cells infected by the WT (Fig. 6a). Through the quantification of stained methylene blue on infected HeLa cells relative to noninfected cells, our results indicate that the mutation of *ppk* significantly reduced the ability of SP15 to induce megalocytosis, which was restored in SP15 Δ*ppk*-c (Fig. 6b). This indicates that PPK is required for colibactin-producing *E. coli* to induce DNA damage and subsequent megalocytosis of host cells.

Mesalamine reduces P*clbB* activity and represses colibactin production. One well-known PPK enzymatic activity inhibitor is the anti-inflammatory drug mesalamine, commonly prescribed for IBD and proposed for CRC prevention (25). We thus investigated whether mesalamine has an effect on colibactin synthesis similar to what we observed in Δ*ppk* mutants. First, we tested the effect of mesalamine on P*clbB* activity in two genetic backgrounds, SP15 and EcN. Luminescence emitted by the bacteria was monitored in DMEM-HEPES at 37°C with or without the presence of mesalamine (2 or 4 mM). The results showed that mesalamine reduced P*clbB* activity in a dose-dependent manner in both SP15 (Fig. 7a and b) and EcN (Fig. 7c and d), while it did not cause growth retardation of bacteria (Fig. S3). This indicates that mesalamine has an inhibitory effect on P*clbB* activity.

To test whether mesalamine treatment has an impact on the production of colibactin, we quantified the production of the prodrug motif C_{14}AsnOH of the bacteria with or without mesalamine. We observed that a dose of 8 mM mesalamine decreased

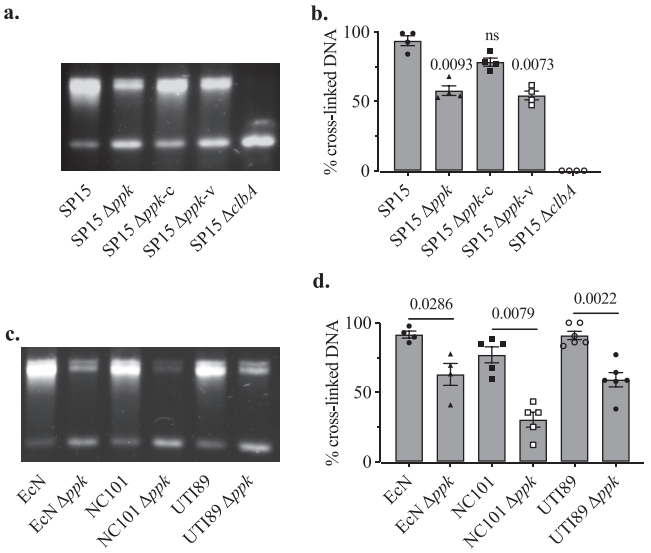


FIG 3 Deletion of *ppk*-reduced ICL amount induced by colibactin-producing *E. coli*. (a) DNA interstrand cross-link (ICL) formation caused by SP15, SP15 Δ*ppk*, the complemented strain SP15 Δ*ppk* carrying plasmid pGEN-*ppk* expressing *ppk* (SP15 Δ*ppk*-c), the control SP15 Δ*ppk* carrying the vector pGEN-MCS (SP15 Δ*ppk*-v), and the negative-control *clbA*-deletion mutant (SP15 Δ*clbA*). The DNA with ICL is nondenaturable and displays delayed migration (upper band) compared to the unaffected denatured single-stranded DNA (lower band). This image is representative of those from four independent experiments. (b) The percentage of the cross-linked DNA signal in the upper band relative to the total DNA signal in the lane was determined by image analysis. Bars represent means ± SEMs ($n = 4$ biological replicates). The significance of the difference between each strain and the WT was determined using the Kruskal-Wallis test followed by the two-stage step-up method of Benjamini, Krieger, and Yekutieli; *P* values are shown. ns, no significant difference. (c) ICL activity of WT strains EcN, NC101, and UTI89 and their respective *ppk* deletion mutants EcN Δ*ppk*, NC101 Δ*ppk*, and UTI89 Δ*ppk*. This image is representative of those from four independent experiments. (d) Percentage of cross-linked DNA signal relative to the total DNA signal in panel c. Bars represent means ± SEMs ($n = 4$ to 6 biological replicates). The significance of the difference between the Δ*ppk* mutant and the WT was determined using the Mann-Whitney test; *P* values are shown.

about 6 times the C_{14}AsnOH level (Fig. 8) without affecting bacterial viability (Fig. S4). This result indicates that mesalamine inhibits the biosynthesis of colibactin.

We investigated the effect of mesalamine on ICL formation induced by various colibactin-producing *E. coli* strains, including SP15 (Fig. 9a and b), EcN (Fig. 9c and d), NC101 (Fig. 9e and f), and UTI89 (Fig. 9g and h). We observed that a dose of 15 mM mesalamine significantly reduced ICL formation in all the strains tested, while the bacterial CFU were not reduced and even showed a slight increase with the treatment with mesalamine (Fig. S5). To confirm these results, we also evaluated the genotoxicity in eukaryotic cells induced by colibactin-producing *E. coli* with or without mesalamine treatment. By using ICW assays, we observed that the genotoxicity induced by SP15

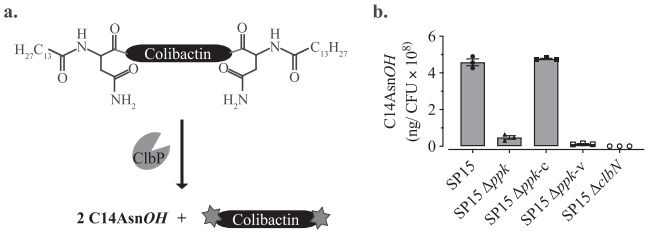


FIG 4 Deletion of *ppk* reduced the production of colibactin. (a) ClbP cleaves the amide bonds of precolibactin to release the prodrug motif C_{14}AsnOH and active colibactin (3). (b) The amount of C_{14}AsnOH produced by SP15 and the derivatives was quantified by liquid chromatography-mass spectrometry (LC-MS). Bacteria were cultivated in DMEM-HEPES at 37°C for 8 h, and C_{14}AsnOH in the supernatant was quantified. The results were normalized to CFU and are presented as the quantity of C_{14}AsnOH. The bars represent means ± SEMs ($n = 3$ biological replicates).

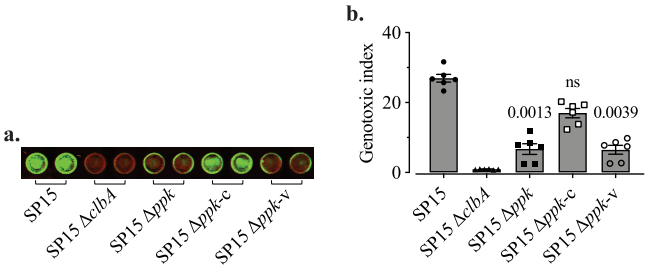


FIG 5 Deletion of *ppk* reduces the genotoxicity of colibactin-producing *E. coli* in eukaryotic cells. (a) HeLa cells after a transient infection with SP15, SP15 Δ*ppk*, SP15 Δ*ppk*-c, SP15 Δ*ppk*-v, or SP15 Δ*clbA*. The multiplicity of infection (MOI) was 100. The signal of γH2AX is pseudocolored in green and the signal of DNA in red. This image is representative of those from three independent experiments performed with two independent bacterial cultures. (b) The genotoxic index was determined by quantification of the signal of γH2AX relative to DNA content and normalized to the control without infection. Bars represent means ± SEMs ($n = 6$ independent experimental replicates). The significance of the difference between each strain and WT was determined using the Kruskal-Wallis test followed by the two-stage step-up method of Benjamini, Krieger, and Yekutieli; *P* values are shown.

was reduced in a dose-dependent manner with the treatment of mesalamine (Fig. 10), while the viability of HeLa cells was not affected (Fig. S6a), and the bacterial CFU were not reduced, by mesalamine (Fig. S6b). Taken together, these results demonstrated that treatment with mesalamine inhibited the production of colibactin, thereby protecting eukaryotic cells from the genotoxicity of colibactin-producing *E. coli*.

We then investigated the impact of mesalamine treatment in a Δ*ppk* mutant on P*clbB* activity, colibactin production, and genotoxicity. We observed that mesalamine decreased P*clbB* activity (Fig. S7a and b), the production level of C_{14}AsnOH (Fig. S7d), and genotoxicity (Fig. S7f and g), without reducing bacterial viability (Fig. S7c, e, and h). These results indicate that mesalamine inhibits P*clbB* activity and colibactin production independently from its inhibition effect on PPK enzymatic activity (25).

DISCUSSION

The data implicating colibactin in virulence and colorectal tumorigenesis have motivated extensive structural and pharmacological studies of colibactin (5, 28–33) and other metabolites of the *pks* pathway (2, 34, 35). However, very limited data are available about the regulation of the production of this important genotoxin. In this study, we developed a high-throughput screening of regulators involved in colibactin biosyn-

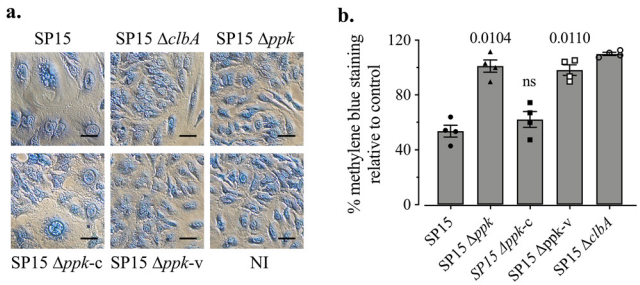


FIG 6 Deletion of *ppk* abolished the ability of colibactin-producing *E. coli* to induce megalocytosis of eukaryotic cells. (a) HeLa cells stained with methylene blue after a transient infection with SP15 Δ*ppk*-c, SP15 Δ*ppk*-v, or SP15 Δ*clbA* at an MOI of 100. NI, not infected. The scale bars represent 50 μm. After a 4-h infection, HeLa cells were washed and incubated for 72 h in the presence of gentamicin. Then, the cells were fixed and stained with methylene blue. This image is representative of those from 4 independent experiments. (b) The cell viability relative to that of NI controls was determined by quantification of methylene blue staining. The methylene blue was extracted and quantified by the measurement of OD_{660}. Bars represent means ± SEMs ($n = 4$ independent experimental replicates). The significance of the difference between each strain and the WT was determined using the Kruskal-Wallis test followed by the two-stage step-up method of Benjamini, Krieger, and Yekutieli; *P* values are shown.

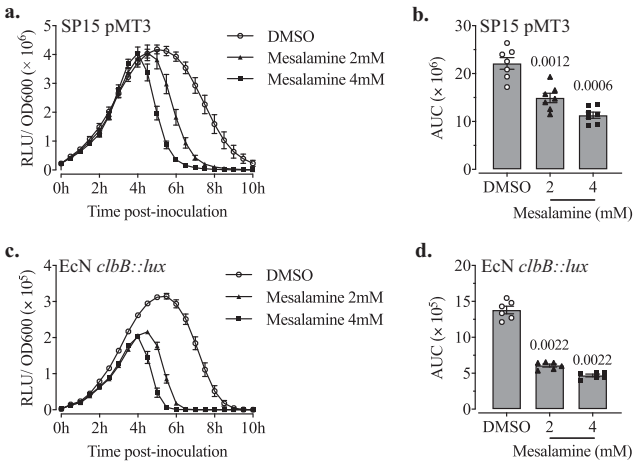


FIG 7 Mesalamine treatment reduces P*clbB* activity. (a) Time course RLU/OD_{600} of SP15(pMT3) with the treatment of mesalamine (2 mM and 4 mM) and the solvent DMSO as a control in DMEM-HEPES at 37°C. (b) AUC of RLU/OD_{600} from panel a. The symbol and bars represent means ± SEMs ($n = 7$ biological replicates). The significance compared with the control (DMSO) was determined using the Mann-Whitney test; the *P* value is shown. (c) RLU/OD_{600} of EcN *clbB*::*lux* with treatment and growing conditions as before. (d) AUC of RLU/OD_{600} from panel c. The symbol and bars represent means ± SEMs ($n = 6$ biological replicates). The significance compared with the control (DMSO) was determined using the Mann-Whitney test; the *P* value is shown.

thesis based on the construction of a library of random mutants of a colibactin-producing *E. coli* strain harboring a P*clbB*-reporter fusion. We reasoned that because ClbB is essential for the production of colibactin, regulators of P*clbB* activity should impact the production level of colibactin. Of 823 mutants screened, 1 mutant had lower P*clbB* activity than the WT. This mutant had the transposon inserted in the gene *ppk*, encoding the polyphosphate kinase (PPK). We then constructed isogenic mutants of *ppk* in different colibactin-producing *E. coli* strains to test P*clbB* activity and the production of colibactin as well. Consistently, the deletion of *ppk* reduced P*clbB* activity and caused a lower production level of colibactin.

This work highlights the role of PPK in P*clbB* activity, which is correlated with the production of colibactin. A recent study has shown that ClbR is the transcriptional activator of *clbB* (17). In this work, we discovered the first regulator of *clbB* transcriptional activity outside of the *pks* island. PPK is essential for the production of long-chain polyP (36). *E. coli* mutants lacking *ppk* were described to be defective in virulence and responses to multiple stresses (i.e., nutrient starvation, oxidants, acidic challenge, osmotic shock, and heat shock) (24, 37, 38). Additionally, the *ppk* deletion mutant of meningitis *E. coli* strain E44 showed less ability than the WT to cross the blood-brain barrier (BBB) (37). The *ppk* deletion mutant of the uropathogenic strain UTI89 was

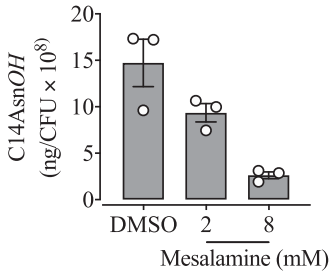


FIG 8 Mesalamine represses colibactin production. Shown is quantification of C_{14}AsnOH produced by SP15 with treatment with mesalamine (2 mM and 8 mM) and the solvent DMSO. Bacteria were cultivated in DMEM-HEPES (in the presence of mesalamine or DMSO) at 37°C for 8 h, and C_{14}AsnOH in the supernatant was quantified. The results were normalized to CFU and are presented as the quantity of C_{14}AsnOH. The bars represent means ± SEMs ($n = 3$ biological replicates).

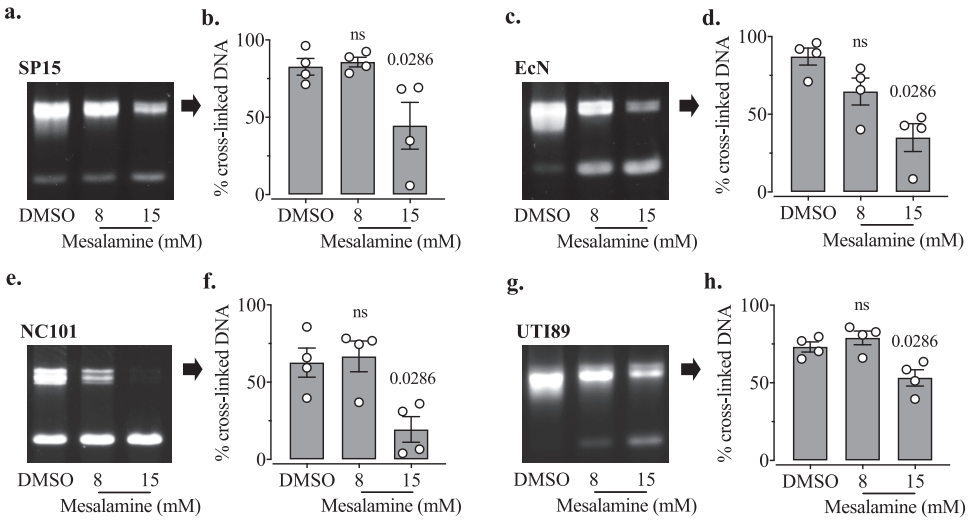


FIG 9 Mesalamine inhibits ICL activity of colibactin-producing *E. coli*. The strains SP15 (a and b), EcN (c and d), NC101 (e and f), and UTI89 (g and h) were inoculated at 1.5×10^6 CFU in 100 μl of DMEM-HEPES, with treatment with mesalamine (8 mM and 15 mM), and the solvent DMSO (control, 4% end concentration, similar to the end concentration of DMSO in samples treated with 15 mM mesalamine). After 4 h of incubation at 37°C, bacteria were spun down and resuspended with sterile Milli-Q H_2O. Then, 500 ng of linearized pUC19 plasmid was added into each resuspension. After 40 min of incubation at 37°C, DNA was purified, loaded onto an agarose gel, and migrated under alkaline denaturing conditions. DNA with covalent ICLs is nondenaturable and displays delayed migration compared to denatured single-stranded DNA (lower band). The percentage of the DNA signal in the upper (cross-linked DNA band) relative to the total DNA signal in the lane was determined by image analysis. (c, e, and g) The photos are representative of those from four experiments. (d, f, and h) The quantifications of cross-linked DNA were determined as previously described. The bars represent means ± SEMs ($n = 4$ independent experimental replicates). The significance compared with the control (DMSO) was determined using the Mann-Whitney test; the *P* value is shown.

shown to have defects in biofilm formation, resistance to oxidation, and formation of antibiotic-resistant persister cells (25, 39). PPK is distributed across a wide spectrum of bacterial pathogens and absent in mammalian cells, and it has been therefore proposed as a new target for developing antibacterial agents that specifically target pathogens without affecting the host and its beneficial bacteria (40). In this work, we observed the deletion of *ppk* reduced the genotoxicity of colibactin-producing *E. coli*, including the meningitic strain SP15, the probiotic strain EcN, the colitogenic strain NC101, and the uropathogenic strain UTI89. Future research should clarify whether this is the case *in vivo*. Our finding reinforces the idea to take PPK as a target of antibacterial drugs and provided a new path for developing an anticolibactin strategy.

Several studies have focused on finding inhibitors of PPK (25, 41–43). One of the iden-

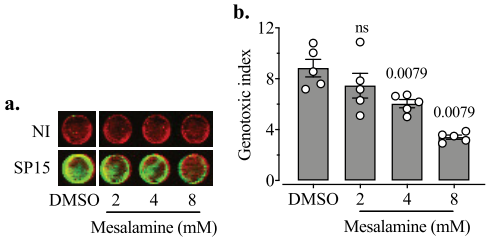


FIG 10 Mesalamine inhibits the genotoxicity of colibactin-producing *E. coli*. (a) HeLa cells after a transient infection with SP15 under the treatment with mesalamine (2 mM, 4 mM, or 8 mM) and the solvent DMSO (control). The MOI was 100. The signal of γH2AX is green, and the signal of DNA is red. This image is representative of those from four independent experiments. (b) The genotoxic index was determined by quantification of the signal of γH2AX relative to DNA content and normalized to the control without infection. The bars represent means ± SEMs ($n = 5$ independent experimental replicates). The significance of the difference between each strain and the control was determined using the Kruskal-Wallis test followed by the two-stage step-up method of Benjamini, Krieger, and Yekutieli; *P* values of <0.05 are shown.

tified PPK inhibitors, mesalamine (also known as mesalazine or 5-aminosalicylic acid), has been validated by treating different bacteria ranging from clinically isolated uropathogenic *E. coli* and *P. aeruginosa* strains to human gastrointestinal luminal samples (25). Mesalamine is a drug commonly used to treat IBD patients, and rare side effects have been reported (44–46). Mesalamine exerts its anti-inflammatory effects locally on the colorectal mucosa, and the efficacy is dependent on achieving high intraluminal concentrations (47, 48). In patients conventionally treated with mesalamine, stool concentrations of mesalamine are on the median order of 30 mM, ranging from 10 to 100 mM; these concentrations correspond to luminal concentrations of mesalamine 100 times greater than the concentrations in the colonic mucosa (49). Mesalamine has been shown to have chemopreventive effects on CRC and has been proposed as a first-line treatment that should be given daily in high doses and long term to reduce the possibility of recurrence and risk of CRC (45, 50, 51). The effects of mesalamine on the host have been intensely researched (51–56), while few studies have investigated the effects on bacteria. Mesalamine has been shown to affect bacterial gene expression (49) and to alter gut microbiota (57–59). Interestingly, a recent report showed that mesalamine downregulated the transcription of the *pks* gene (60), but it did not show which *pks* gene was downregulated. This study also showed that mesalamine (9.8 mM and 13 mM) inhibited DNA breakage in colonic epithelial Caco-2 cells induced by colibactin-producing *E. coli* (60). In our study, we first identified PPK as an enhancer of colibactin production, which led us to test the PPK inhibitor mesalamine. We tested not only the inhibitory effects of mesalamine on the genotoxicity of colibactin-producing *E. coli* in eukaryotic cells but also directly the amount of colibactin-correlated metabolite C_{14}AsnOH and the formation of ICL. We also tested a wider range of colibactin-producing *E. coli* strains and demonstrated that the effect of mesalamine on colibactin production is universal. Among the strains tested, one strain should especially get our attention: the probiotic strain EcN, which is the active component of microbial drug Mutaflor (61). EcN has been widely used in the treatment of IBD and has proven to be as effective as the gold standard mesalamine for the maintenance of remission in ulcerative colitis patients (61). It has been suggested that a combination of mesalamine and EcN might exert additive or synergistic therapeutic efficacy, and mesalamine has no effect on the viability of EcN *in vivo* (62). Here, our data suggest that *in vitro* mesalamine has a suppressive effect on the genotoxicity of EcN without altering the viability of EcN. Future research should clarify whether this is the case *in vivo*.

In this study, we also investigated whether mesalamine treatment inhibits the biosynthesis of colibactin in a Δ*ppk* mutant. Interestingly, an additional inhibition effect on colibactin production was observed in the Δ*ppk* mutant treated with mesalamine, indicating that mesalamine is capable of inhibiting colibactin production independently from its inhibitory effect on PPK enzymatic activity (25). Future research is needed to clarify this new mechanism.

In summary, this study showed that PPK played a role in the transcriptional activity of *clbB* and was required for the genotoxicity of colibactin-producing *E. coli*. This provided us a new perspective on the regulatory network of colibactin production and brought us a novel clue for anticolibactin strategy development. By using the PPK inhibitor mesalamine, we confirmed the role of PPK in colibactin production and also identified mesalamine as an effective drug for inhibiting *pks*$^+$ *E. coli* genotoxicity to eukaryotic cells. Further studies are necessary to test the synergistic activity of mesalamine and EcN *in vivo* and to determine if treatment of IBD with both mesalamine and EcN protects patients against CRC.

MATERIALS AND METHODS

Bacterial strains, plasmids, and growth conditions. The bacterial strains and plasmids used in this study are listed in Table 1. Gene mutagenesis was performed by using the λ red mutagenesis method with the primers listed in Table 2 and confirmed by PCR. For genetic manipulations, all *E. coli* strains were grown routinely in lysogenic broth (LB) medium. When appropriate, antibiotics were added at the following concentrations: 50 μg/ml for kanamycin, 50 μg/ml for carbenicillin, and 25 μg/ml for chloramphenicol.

TABLE 2 Primers used in this study

Primer	Sequence (5′–3′)[a]	Aim
MT3_P*clbB*-EcoRI-F	CCGGAATTCCTTTGAACTTATCCATGTTTCC	Cloning of DNA sequence MT3 containing the promoter of *clbB*
MT1_P*clbB*-BamHI-R	CGCGGATCCCAGAGGTATTATCCATAACCATCAC	
MT43_*ppk*-mut-F	CGCCATAATATCCAGGCAGTGTCCCGTGAATAAAACGGA GTAAAAGTGGTA**TGTGTAGGCTGGAGCTGCTTCG**	Deletion of *ppk*
MT44_*ppk*-mut-R	GTTATTCAGATTGTTCGAGTGATTTGATGTAGTCGTAAAT CGCCAACTGCG**CATATGAATATCCTCCTTAGTTC**	
MT54_pGEN-*ppk*-HindIII-F	CCGAAGCTTGTACATCGGTGCATTTCGTC	Amplification of *ppk* plus its putative promoter region
MT55_pGEN-*ppk*-BamHI-R	CGCGGATCCAGGGTTATTCAGATTGTTCGAG	

[a]Restriction enzyme sites are underlined, and priming sites for amplifying resistance gene are written in bold.

Chemicals and reagents. Unless otherwise indicated, chemicals were from Sigma-Aldrich or Fisher. The stock solution of mesalamine (400 mM) was extemporaneously prepared in dimethyl sulfoxide (DMSO), and dilutions were made immediately before each experiment.

Plasmid construction. The plasmids used in this study are listed in Table 1. For the construction of *clbB* promoter (P*clbB*) reporter fusions, the promoter sequence of *clbB* (from bp −473 to +17 relative to the initiation start codon of *clbB*), 490 bp, named MT3, containing P*clbB* was amplified from the genome of SP15 and cloned into the reporter plasmid pCM17 preceding the *luxCDABE* operon (Fig. S1). The primers used are listed in Table 2. The result plasmid, pMT3, was verified by sequencing. After pMT3 is introduced into the target bacteria, the *luxCDABE* operon encodes a luciferase (LuxA and LuxB) and the enzymes that produce its substrate (LuxC, LuxD, and LuxE) under the control of P*clbB*, so bacteria that have P*clbB* activated and express the cluster emit 490-nm luminescence spontaneously. The promoter-reporter fusion pMT3 contains the kanamycin resistance (Kan^r) cassette. For compatibility with the transposon containing the Kan^r cassette, the Kan^r cassette of pMT3 was disrupted by inserting an ampicillin resistance (Amp^r) gene at the restriction site BssHII, which resulted in pMT3a. The plasmids were verified by sequencing. For complementation, the coding sequence of gene *ppk* plus its putative promoter region was amplified (the primers used are listed in Table 2) and cloned into pGEN-MCS using HindIII and BamHI restriction sites. All restriction enzymes were purchased from New England BioLabs (NEB) and used based on the supplier's recommendations.

Construction of Tn mutant library and identification of Tn insertion sites of selected mutants. The transposon (Tn) mutant library of *E. coli* strain SP15 containing pMT3a was prepared using the EZ-Tn5 <KAN-2>Tnp Transposome kit (Lucigen). Mutants were stored at –80°C with 20% (vol/vol) glycerol as a cryoprotectant. To identify Tn insertion sites of selected mutants, DNA fragments spanning the Tn insertion junction were amplified by arbitrarily primed PCR (AP-PCR) for sequence analysis (63), and then the resulting sequence was mapped to the bacterial genome and plasmids.

Luminescence measurement. For monitoring *clbB* promoter (P*clbB*) activity in SP15 (carrying pMT3a or pMT3) and the mutants, each strain was inoculated into 150 μl of LB and grown at 37°C without shaking. A total of 5 μl of overnight culture was inoculated into 100 μl of Dulbecco's modified Eagle's medium (DMEM)-HEPES (Gibco) in a black 96-well plate (Greiner Bio-One), and then the bacteria were grown without shaking at 37°C. The luminescence emission (relative light units [RLU]; 2,000-ms aperture per sample) and the optical density at 600 nm (OD_{600}) were measured at 4 h by a luminometer (Tecan Spark multimode reader). To have the time course P*clbB* activity, the bacteria were grown without shaking at 37°C in the luminometer, and RLU and OD_{600} were measured every 0.5 h. The area under the curve (AUC) of RLU/OD_{600}, which quantifies the cumulative luminescence, was calculated with GraphPad Prism (version 8.0) software.

To monitor P*clbB* activity in EcN *clbB*::*lux* (Fig. S1b) (17, 26) and the derivatives, each strain was inoculated into 3 ml of LB and grown at 37°C with shaking at 240 rpm overnight. A total of 500 μl of overnight culture was inoculated into 9.5 ml of DMEM-HEPES and then grown at 37°C with shaking at 240 rpm for 8h. Ten-microliter subcultures were inoculated into 100 μl of DMEM-HEPES in a black 96-well plate. Bacteria were grown without shaking at 37°C in the luminometer, and RLU and OD_{600} were measured at 0.5 h. The AUC was determined as previously described. To detect the effect of mesalamine on P*clbB* activity in EcN and SP15, the same protocol was used; mesalamine was added in 100 μl of DMEM-HEPES in the black 96-well plate inoculated with 10-μl subcultures.

C_{14}AsnOH (colibactin cleavage product) quantification. Each *E. coli* strain was inoculated in triplicate into 3 ml of LB and grown at 37°C with shaking at 240 rpm overnight. A total of 500 μl of overnight culture was inoculated into 9.5 ml of DMEM-HEPES and then grown at 37°C with shaking at 240 rpm to an optical density at OD_{600} of 0.4 to ~0.6. Then 500 μl of subculture was inoculated into 9.5 ml of DMEM-HEPES and grown under the same condition for 8 h. Bacterial cells were pelleted by centrifugation at 5,000 × *g* for 10 min, and the supernatants were filtered through a 0.22-μm-pore-size polyvinylidene difluoride (PVDF) filter (Millipore). The supernatants were stored at –80°C until *N*-myristoyl-D-asparagine (C_{14}AsnOH) extraction. With the same protocol for lipid extraction as previously described (34), 5 μl of internal standard (IS) mixture (deuterium-labeled compounds) (400 ng/ml) and 0.3 ml of cold methanol (MeOH) was added to each 1-ml supernatant sample. An Oasis HLB 96-well plate was conditioned with 500 μl of MeOH and 500 μl of 10% MeOH/H_2O. The samples were loaded in this conditioned plate and then washed with 500 μl of 10% MeOH/H_2O and dried under aspiration. Lipids were eluted with 750 μl of MeOH, evaporated twice under N_2, and then suspended in 10 μl of methanol. The quantification of C_{14}AsnOH was performed by the MetaToul Lipidomics Facility (Inserm UMR1048, Toulouse,

France), using an in-house quantification assay by high-performance liquid chromatography/tandem mass spectrometry analysis.

Genotoxicity assay. HeLa cells (1.5×10^5/200 μl/well) were grown in DMEM GlutaMAX supplemented with 10% fetal calf serum (FCS) and 1% nonessential amino acids (NEAA), in 96-well culture plates, at 37°C in a 5% CO_2 incubator for 24 h. Each *E. coli* strain was inoculated into 3 ml of LB and grown at 37°C with shaking at 240 rpm overnight. A total of 500 μl of overnight culture was inoculated into 9.5 ml of DMEM-HEPES and then grown at 37°C with shaking at 240 rpm to an OD_{600} of 0.4 to ~0.6. Then HeLa cells were infected at a multiplicity of infection (MOI) of 100, 50, 25, or 12.5 with each strain with or without mesalamine. At 4 h postinfection, the cells were washed 3 times with Hanks' balanced salt solution (HBSS) and incubated at 37°C in DMEM GlutaMAX supplemented with FCS and NEAA for 3 h with 200 μg/ml of gentamicin. The in-cell Western (ICW) procedure was performed as previously described (2). Briefly, after cells were fixed, permeabilized, and blocked, they were incubated overnight at 4°C with rabbit monoclonal anti-γH2AX antibody 9718 (Cell Signaling Technology; 1:200). An infrared fluorescent secondary antibody absorbing at 800 nm (IRDye 800CW, 1:500; Rockland Immunochemicals) was then applied. DNA was counterstained with RedDot2 (Biotium; 1:500). DNA and γH2AX were visualized simultaneously using an Odyssey infrared imaging scanner (LI-COR Biosciences) at 680 nm and 800 nm. Relative fluorescent units for γH2AX per well (as determined by the 800-nm signal divided by the 700-nm signal) were divided by untreated controls to determine the genotoxic index.

DNA cross-linking assay. The assay was performed as previously described (27). Briefly, linearized DNA was obtained by digesting plasmid pUC19 with BamHI (NEB). Each *E. coli* strain was inoculated into 3 ml of LB and grown at 37°C with shaking at 240 rpm overnight. A total of 500 μl of overnight culture was inoculated into 9.5 ml of DMEM-HEPES and then grown at 37°C with shaking at 240 rpm to an OD_{600} of 0.4 to ~0.6. For bacterium-DNA interactions, 1.5×10^6 bacteria were inoculated into 100 μl of DMEM-HEPES with or without mesalamine for 4 h at 37°C without shaking. Following centrifugation for 10 min at 5,000 $\times$ *g*, bacteria were pelleted and resuspended in sterile Milli-Q H_2O. Then, 500 ng of linearized DNA was added into the bacterial suspension and incubated for 40 min at 37°C without shaking. The bacteria were then pelleted by centrifugation for 5 min at 5,000 $\times$ *g*, and the DNA was extracted from the supernatant by purification using a PCR purification kit (Qiagen) according to the manufacturer's recommendations.

A denaturing agarose gel was prepared by dissolving 1.0 g of agarose in 100 ml of a 100 mM NaCl and 2 mM EDTA solution (pH 8.0). The gel was then soaked (2 h) in an alkaline running buffer solution (40 mM NaOH and 1 mM EDTA [pH ~12.0]). A total of 100 ng of each DNA sample was loaded onto the agarose gel. The gel was run for 45 min at 1 V/cm and then 2 h at 2 V/cm. The gel was then neutralized for a total of 45 min in a 100 mM Tris (pH 7.4) buffer solution containing 150 mM NaCl. The gel was stained with GelRed for 20 min and revealed with UV exposure using the ChemiDoc imaging system (Bio-Rad).

Megalocytosis assay. Quantification of the colibactin-associated genotoxic effect by megalocytosis assay was performed as previously described (1). Briefly, HeLa cells (5×10^3/well) were grown in DMEM GlutaMAX (Gibco) supplemented with 10% (vol/vol) FCS (Eurobio) and 1% (vol/vol) NEAA (Invitrogen), in 96-well culture plates, at 37°C in a 5% CO_2 incubator for 24 h. Each *E. coli* strain was inoculated into 3 ml of LB and grown at 37°C with shaking at 240 rpm overnight. A total of 500 μl of overnight culture was inoculated into 9.5 ml of DMEM-HEPES and then grown at 37°C with shaking at 240 rpm to an OD_{600} of 0.4 to ~0.6. Then HeLa cells were infected at MOIs of 100 and 50 with each strain in 100 μl of DMEM-HEPES. At 4 h postinfection, the cells were washed 3 times with HBSS (Gibco) and incubated in DMEM GlutaMAX supplemented with FCS, NEAA, and 200 mg/ml of gentamicin for 72 h before fixation (4% formaldehyde) and protein staining with methylene blue (1% [wt/vol] in 0.01 M Tris-HCl). The methylene blue was extracted with 0.1 M HCl. Staining was quantified by measurement of the OD_{660}.

Statistical analyses. The mean and the standard error of the mean (SEM) are shown in the figures, unless otherwise stated. *P* values were calculated in GraphPad Prism 8.0 by the Mann-Whitney test or Kruskal-Wallis test followed by the two-stage step-up method of Benjamini, Krieger, and Yekutieli. *P* values of <0.05 were considered statistically significant.

SUPPLEMENTAL MATERIAL

Supplemental material is available online only.

FIG S1, EPS file, 0.7 MB.

FIG S2, EPS file, 0.6 MB.

FIG S3, EPS file, 0.1 MB.

FIG S4, EPS file, 0.1 MB.

FIG S5, EPS file, 0.6 MB.

FIG S6, EPS file, 0.1 MB.

FIG S7, EPS file, 2.1 MB.

ACKNOWLEDGMENTS

This work was supported by grants from the French National Agency for Research (ANR) (UTI-TOUL ANR-17-CE35-0010).

We thank Nicolas Cenac and Julien Pujo for helping with lipid extraction, Patricia Martin for offering control strains, Matteo Serino for helping with statistical analysis,

and Marion Garofalo for helping read fluorescence in ICW assay. We also thank the lipidomic facility of MetaToul, Toulouse, France.

REFERENCES

1. Nougayrede JP, Homburg S, Taieb F, Boury M, Brzuszkiewicz E, Gottschalk G, Buchrieser C, Hacker J, Dobrindt U, Oswald E. 2006. Escherichia coli induces DNA double-strand breaks in eukaryotic cells. Science 313:848–851. https://doi.org/10.1126/science.1127059.
2. Martin P, Marcq I, Magistro G, Penary M, Garcie C, Payros D, Boury M, Olier M, Nougayrede JP, Audebert M, Chalut C, Schubert S, Oswald E. 2013. Interplay between siderophores and colibactin genotoxin biosynthetic pathways in Escherichia coli. PLoS Pathog 9:e1003437. https://doi.org/10.1371/journal.ppat.1003437.
3. Brotherton CA, Balskus EP. 2013. A prodrug resistance mechanism is involved in colibactin biosynthesis and cytotoxicity. J Am Chem Soc 135:3359–3362. https://doi.org/10.1021/ja312154m.
4. Pleguezuelos-Manzano C, Puschhof J, Rosendahl Huber A, van Hoeck A, Wood HM, Nomburg J, Gurjao C, Manders F, Dalmasso G, Stege PB, Paganelli FL, Geurts MH, Beumer J, Mizutani T, Miao Y, van der Linden R, van der Elst S, Genomics England Research C, Garcia KC, Top J, Willems RJL, Giannakis M, Bonnet R, Quirke P, Meyerson M, Cuppen E, van Boxtel R, Clevers H, Genomics England Research Consortium. 2020. Mutational signature in colorectal cancer caused by genotoxic pks(+) E. coli. Nature 580:269–273. https://doi.org/10.1038/s41586-020-2080-8.
5. Xue M, Wernke KM, Herzon SB. 2020. Depurination of colibactin-derived interstrand cross-links. Biochemistry 59:892–900. https://doi.org/10.1021/acs.biochem.9b01070.
6. Dziubańska-Kusibab PJ, Berger H, Battistini F, Bouwman BAM, Iftekhar A, Katainen R, Cajuso T, Crosetto N, Orozco M, Aaltonen LA, Meyer TF. 2020. Colibactin DNA-damage signature indicates mutational impact in colorectal cancer. Nat Med 26:1063–1069. https://doi.org/10.1038/s41591-020-0908-2.
7. McCarthy AJ, Martin P, Cloup E, Stabler RA, Oswald E, Taylor PW. 2015. The genotoxin colibactin is a determinant of virulence in Escherichia coli K1 experimental neonatal systemic infection. Infect Immun 83:3704–3711. https://doi.org/10.1128/IAI.00716-15.
8. Marcq I, Martin P, Payros D, Cuevas-Ramos G, Boury M, Watrin C, Nougayrede JP, Olier M, Oswald E. 2014. The genotoxin colibactin exacerbates lymphopenia and decreases survival rate in mice infected with septicemic Escherichia coli. J Infect Dis 210:285–294. https://doi.org/10.1093/infdis/jiu071.
9. Tronnet S, Floch P, Lucarelli L, Gaillard D, Martin P, Serino M, Oswald E. 2020. The genotoxin colibactin shapes gut microbiota in mice. mSphere 5:e00589-20. https://doi.org/10.1128/mSphere.00589-20.
10. Cuevas-Ramos G, Petit CR, Marcq I, Boury M, Oswald E, Nougayrede JP. 2010. Escherichia coli induces DNA damage in vivo and triggers genomic instability in mammalian cells. Proc Natl Acad Sci U S A 107:11537–11542. https://doi.org/10.1073/pnas.1001261107.
11. Payros D, Secher T, Boury M, Brehin C, Menard S, Salvador-Cartier C, Cuevas-Ramos G, Watrin C, Marcq I, Nougayrede JP, Dubois D, Bedu A, Garnier F, Clermont O, Denamur E, Plaisancie P, Theodorou V, Fioramonti J, Olier M, Oswald E. 2014. Maternally acquired genotoxic Escherichia coli alters offspring's intestinal homeostasis. Gut Microbes 5:313–325. https://doi.org/10.4161/gmic.28932.
12. Dejea CM, Fathi P, Craig JM, Boleij A, Taddese R, Geis AL, Wu X, DeStefano Shields CE, Hechenbleikner EM, Huso DL, Anders RA, Giardiello FM, Wick EC, Wang H, Wu S, Pardoll DM, Housseau F, Sears CL. 2018. Patients with familial adenomatous polyposis harbor colonic biofilms containing tumorigenic bacteria. Science 359:592–597. https://doi.org/10.1126/science.aah3648.
13. Dalmasso G, Cougnoux A, Delmas J, Darfeuille-Michaud A, Bonnet R. 2014. The bacterial genotoxin colibactin promotes colon tumor growth by modifying the tumor microenvironment. Gut Microbes 5:675–680. https://doi.org/10.4161/19490976.2014.969989.
14. Cougnoux A, Dalmasso G, Martinez R, Buc E, Delmas J, Gibold L, Sauvanet P, Darcha C, Dechelotte P, Bonnet M, Pezet D, Wodrich H, Darfeuille-Michaud A, Bonnet R. 2014. Bacterial genotoxin colibactin promotes colon tumour growth by inducing a senescence-associated secretory phenotype. Gut 63:1932–1942. https://doi.org/10.1136/gutjnl-2013-305257.
15. Arthur JC, Perez-Chanona E, Muhlbauer M, Tomkovich S, Uronis JM, Fan TJ, Campbell BJ, Abujamel T, Dogan B, Rogers AB, Rhodes JM, Stintzi A, Simpson KW, Hansen JJ, Keku TO, Fodor AA, Jobin C. 2012. Intestinal inflammation targets cancer-inducing activity of the microbiota. Science 338:120–123. https://doi.org/10.1126/science.1224820.
16. Dubinsky V, Dotan I, Gophna U. 5 June 2020. Carriage of colibactin-producing bacteria and colorectal cancer risk. Trends Microbiol https://doi.org/10.1016/j.tim.2020.05.015.
17. Wallenstein A, Rehm N, Brinkmann M, Selle M, Bossuet-Greif N, Sauer D, Bunk B, Sproer C, Wami HT, Homburg S, von Bunau R, Konig S, Nougayrede JP, Overmann J, Oswald E, Muller R, Dobrindt U. 2020. ClbR is the key transcriptional activator of colibactin gene expression in Escherichia coli. mSphere 5:e00591-20. https://doi.org/10.1128/mSphere.00591-20.
18. Tronnet S, Garcie C, Rehm N, Dobrindt U, Oswald E, Martin P. 2016. Iron homeostasis regulates the genotoxicity of Escherichia coli that produces colibactin. Infect Immun 84:3358–3368. https://doi.org/10.1128/IAI.00659-16.
19. Tronnet S, Garcie C, Brachmann AO, Piel J, Oswald E, Martin P. 2017. High iron supply inhibits the synthesis of the genotoxin colibactin by pathogenic Escherichia coli through a non-canonical Fur/RyhB-mediated pathway. Pathog Dis 75:ftx066. https://doi.org/10.1093/femspd/ftx066.
20. Hancock V, Seshasayee AS, Ussery DW, Luscombe NM, Klemm P. 2008. Transcriptomics and adaptive genomics of the asymptomatic bacteriuria Escherichia coli strain 83972. Mol Genet Genomics 279:523–534. https://doi.org/10.1007/s00438-008-0330-9.
21. Yang Y, Gharaibeh RZ, Newsome RC, Jobin C. 2020. Amending microbiota by targeting intestinal inflammation with TNF blockade attenuates development of colorectal cancer. Nat Cancer 1:723–734. https://doi.org/10.1038/s43018-020-0078-7.
22. Arthur JC, Gharaibeh RZ, Muhlbauer M, Perez-Chanona E, Uronis JM, McCafferty J, Fodor AA, Jobin C. 2014. Microbial genomic analysis reveals the essential role of inflammation in bacteria-induced colorectal cancer. Nat Commun 5:4724. https://doi.org/10.1038/ncomms5724.
23. Prorok-Hamon M, Friswell MK, Alswied A, Roberts CL, Song F, Flanagan PK, Knight P, Codling C, Marchesi JR, Winstanley C, Hall N, Rhodes JM, Campbell BJ. 2014. Colonic mucosa-associated diffusely adherent afaC+ Escherichia coli expressing lpfA and pks are increased in inflammatory bowel disease and colon cancer. Gut 63:761–770. https://doi.org/10.1136/gutjnl-2013-304739.
24. Rao NN, Gomez-Garcia MR, Kornberg A. 2009. Inorganic polyphosphate: essential for growth and survival. Annu Rev Biochem 78:605–647. https://doi.org/10.1146/annurev.biochem.77.083007.093039.
25. Dahl JU, Gray MJ, Bazopoulou D, Beaufay F, Lempart J, Koenigsknecht MJ, Wang Y, Baker JR, Hasler WL, Young VB, Sun D, Jakob U. 2017. The anti-inflammatory drug mesalamine targets bacterial polyphosphate accumulation. Nat Microbiol 2:16267. https://doi.org/10.1038/nmicrobiol.2016.267.
26. Homburg S, Oswald E, Hacker J, Dobrindt U. 2007. Expression analysis of the colibactin gene cluster coding for a novel polyketide in Escherichia coli. FEMS Microbiol Lett 275:255–262. https://doi.org/10.1111/j.1574-6968.2007.00889.x.
27. Bossuet-Greif N, Vignard J, Taieb F, Mirey G, Dubois D, Petit C, Oswald E, Nougayrede JP. 2018. The colibactin genotoxin generates DNA interstrand cross-links in infected cells. mBio 9:e02393-17. https://doi.org/10.1128/mBio.02393-17.
28. Xue M, Kim CS, Healy AR, Wernke KM, Wang Z, Frischling MC, Shine EE, Wang W, Herzon SB, Crawford JM. 2019. Structure elucidation of colibactin and its DNA cross-links. Science 365:eaax2685. https://doi.org/10.1126/science.aax2685.
29. Wilson MR, Jiang Y, Villalta PW, Stornetta A, Boudreau PD, Carra A, Brennan CA, Chun E, Ngo L, Samson LD, Engelward BP, Garrett WS, Balbo S, Balskus EP. 2019. The human gut bacterial genotoxin colibactin alkylates DNA. Science 363:eaar7785. https://doi.org/10.1126/science.aar7785.
30. Li ZR, Li J, Cai W, Lai JYH, McKinnie SMK, Zhang WP, Moore BS, Zhang W, Qian PY. 2019. Macrocyclic colibactin induces DNA double-strand breaks via copper-mediated oxidative cleavage. Nat Chem 11:880–889. https://doi.org/10.1038/s41557-019-0317-7.
31. Xue M, Shine E, Wang W, Crawford JM, Herzon SB. 2018. Characterization of natural colibactin-nucleobase adducts by tandem mass spectrometry and isotopic labeling. Support for DNA alkylation by cyclopropane ring opening. Biochemistry 57:6391–6394. https://doi.org/10.1021/acs.biochem.8b01023.
32. Vizcaino MI, Crawford JM. 2015. The colibactin warhead crosslinks DNA. Nat Chem 7:411–417. https://doi.org/10.1038/nchem.2221.
33. Healy AR, Wernke KM, Kim CS, Lees NR, Crawford JM, Herzon SB. 2019.

Synthesis and reactivity of precolibactin 886. Nat Chem 11:890–898. https://doi.org/10.1038/s41557-019-0338-2.
34. Perez-Berezo T, Pujo J, Martin P, Le Faouder P, Galano JM, Guy A, Knauf C, Tabet JC, Tronnet S, Barreau F, Heuillet M, Dietrich G, Bertrand-Michel J, Durand T, Oswald E, Cenac N. 2017. Identification of an analgesic lipopeptide produced by the probiotic Escherichia coli strain Nissle 1917. Nat Commun 8:1314. https://doi.org/10.1038/s41467-017-01403-9.
35. Massip C, Branchu P, Bossuet-Greif N, Chagneau CV, Gaillard D, Martin P, Boury M, Sécher T, Dubois D, Nougayrède J-P, Oswald E. 2019. Deciphering the interplay between the genotoxic and probiotic activities of Escherichia coli Nissle 1917. PLoS Pathog 15:e1008029. https://doi.org/10.1371/journal.ppat.1008029.
36. Akiyama M, Crooke E, Kornberg A. 1992. The polyphosphate kinase gene of Escherichia coli. Isolation and sequence of the ppk gene and membrane location of the protein. J Biol Chem 267:22556–22561.
37. Peng L, Luo WY, Zhao T, Wan CS, Jiang Y, Chi F, Zhao W, Cao H, Huang SH. 2012. Polyphosphate kinase 1 is required for the pathogenesis process of meningitic Escherichia coli K1 (RS218). Future Microbiol 7:411–423. https://doi.org/10.2217/fmb.12.3.
38. Gray MJ, Jakob U. 2015. Oxidative stress protection by polyphosphate—new roles for an old player. Curr Opin Microbiol 24:1–6. https://doi.org/10.1016/j.mib.2014.12.004.
39. Cremers CM, Knoefler D, Gates S, Martin N, Dahl JU, Lempart J, Xie L, Chapman MR, Galvan V, Southworth DR, Jakob U. 2016. Polyphosphate: a conserved modifier of amyloidogenic processes. Mol Cell 63:768–780. https://doi.org/10.1016/j.molcel.2016.07.016.
40. Tzeng CM, Kornberg A. 1998. Polyphosphate kinase is highly conserved in many bacterial pathogens. Mol Microbiol 29:381–382. https://doi.org/10.1046/j.1365-2958.1998.00887.x.
41. Burda-Grabowska M, Macegoniuk K, Flick R, Nocek BP, Joachimiak A, Yakunin AF, Mucha A, Berlicki L. 2019. Bisphosphonic acids and related compounds as inhibitors of nucleotide- and polyphosphate-processing enzymes: a PPK1 and PPK2 case study. Chem Biol Drug Des 93:1197–1206. https://doi.org/10.1111/cbdd.13439.
42. Bashatwah RM, Khanfar MA, Bardaweel SK. 2018. Discovery of potent polyphosphate kinase 1 (PPK1) inhibitors using structure-based exploration of PPK1Pharmacophoric [*sic*] space coupled with docking analyses. J Mol Recognit 31:e2726. https://doi.org/10.1002/jmr.2726.
43. Bravo-Toncio C, Alvarez JA, Campos F, Ortiz-Severin J, Varas M, Cabrera R, Lagos CF, Chavez FP. 2016. Dictyostelium discoideum as a surrogate host-microbe model for antivirulence screening in Pseudomonas aeruginosa PAO1. Int J Antimicrob Agents 47:403–409. https://doi.org/10.1016/j.ijantimicag.2016.02.005.
44. Lamb CA, Kennedy NA, Raine T, Hendy PA, Smith PJ, Limdi JK, Hayee B, Lomer MCE, Parkes GC, Selinger C, Barrett KJ, Davies RJ, Bennett C, Gittens S, Dunlop MG, Faiz O, Fraser A, Garrick V, Johnston PD, Parkes M, Sanderson J, Terry H, IBD guidelines eDelphi consensus group, Gaya DR, Iqbal TH, Taylor SA, Smith M, Brookes M, Hansen R, Hawthorne AB. 2019. British Society of Gastroenterology consensus guidelines on the management of inflammatory bowel disease in adults. Gut 68:S1–S106. https://doi.org/10.1136/gutjnl-2019-318484.
45. Hauso O, Martinsen TC, Waldum H. 2015. 5-Aminosalicylic acid, a specific drug for ulcerative colitis. Scand J Gastroenterol 50:933–941. https://doi.org/10.3109/00365521.2015.1018937.
46. Adiga A, Goldfarb DS. 2020. The association of mesalamine with kidney disease. Adv Chronic Kidney Dis 27:72–76. https://doi.org/10.1053/j.ackd.2019.09.002.
47. van de Meeberg MM, Schultheiss JPD, Oldenburg B, Fidder HH, Huitema ADR. 2020. Does the 5-aminosalicylate concentration correlate with the efficacy of oral 5-aminosalicylate and predict response in patients with inflammatory bowel disease? A systematic review. Digestion 101:245–261. https://doi.org/10.1159/000499331.
48. Frieri G, Giacomelli R, Pimpo M, Palumbo G, Passacantando A, Pantaleoni G, Caprilli R. 2000. Mucosal 5-aminosalicylic acid concentration inversely correlates with severity of colonic inflammation in patients with ulcerative colitis. Gut 47:410–414. https://doi.org/10.1136/gut.47.3.410.
49. Kaufman J, Griffiths TA, Surette MG, Ness S, Rioux KP. 2009. Effects of mesalamine (5-aminosalicylic acid) on bacterial gene expression. Inflamm Bowel Dis 15:985–996. https://doi.org/10.1002/ibd.20876.
50. Qiu X, Ma J, Wang K, Zhang H. 2017. Chemopreventive effects of 5-aminosalicylic acid on inflammatory bowel disease-associated colorectal cancer and dysplasia: a systematic review with meta-analysis. Oncotarget 8:1031–1045. https://doi.org/10.18632/oncotarget.13715.
51. Bajpai M, Seril DN, Van Gurp J, Geng X, Alvarez J, Minacapelli CD, Gorin S, Das KK, Poplin E, Cheng J, Amenta PS, Das KM. 2019. Effect of long-term mesalamine therapy on cancer-associated gene expression in colonic mucosa of patients with ulcerative colitis. Dig Dis Sci 64:740–750. https://doi.org/10.1007/s10620-018-5378-8.
52. Rousseaux C, Lefebvre B, Dubuquoy L, Lefebvre P, Romano O, Auwerx J, Metzger D, Wahli W, Desvergne B, Naccari GC, Chavatte P, Farce A, Bulois P, Cortot A, Colombel JF, Desreumaux P. 2005. Intestinal antiinflammatory effect of 5-aminosalicylic acid is dependent on peroxisome proliferator-activated receptor-gamma. J Exp Med 201:1205–1215. https://doi.org/10.1084/jem.20041948.
53. Khare V, Krnjic A, Frick A, Gmainer C, Asboth M, Jimenez K, Lang M, Baumgartner M, Evstatiev R, Gasche C. 2019. Mesalamine and azathioprine modulate junctional complexes and restore epithelial barrier function in intestinal inflammation. Sci Rep 9:2842. https://doi.org/10.1038/s41598-019-39401-0.
54. Reifen R, Nissenkorn A, Matas Z, Bujanover Y. 2004. 5-ASA and lycopene decrease the oxidative stress and inflammation induced by iron in rats with colitis. J Gastroenterol 39:514–519. https://doi.org/10.1007/s00535-003-1336-z.
55. Oh-Oka K, Kojima Y, Uchida K, Yoda K, Ishimaru K, Nakajima S, Hemmi J, Kano H, Fujii-Kuriyama Y, Katoh R, Ito H, Nakao A. 2017. Induction of colonic regulatory T cells by mesalamine by activating the aryl hydrocarbon receptor. Cell Mol Gastroenterol Hepatol 4:135–151. https://doi.org/10.1016/j.jcmgh.2017.03.010.
56. Stolfi C, De Simone V, Pallone F, Monteleone G. 2013. Mechanisms of action of non-steroidal anti-inflammatory drugs (NSAIDs) and mesalazine in the chemoprevention of colorectal cancer. Int J Mol Sci 14:17972–17985. https://doi.org/10.3390/ijms140917972.
57. Andrews CN, Griffiths TA, Kaufman J, Vergnolle N, Surette MG, Rioux KP. 2011. Mesalazine (5-aminosalicylic acid) alters faecal bacterial profiles, but not mucosal proteolytic activity in diarrhoea-predominant irritable bowel syndrome. Aliment Pharmacol Therap 34:374–383. https://doi.org/10.1111/j.1365-2036.2011.04732.x.
58. Xu J, Chen N, Wu Z, Song Y, Zhang YF, Wu N, Zhang F, Ren XH, Liu Y. 2018. 5-Aminosalicylic acid alters the gut bacterial microbiota in patients with ulcerative colitis. Front Microbiol 9:1274. https://doi.org/10.3389/fmicb.2018.01274.
59. Olaisen M, Spigset O, Flatberg A, Granlund AV, Brede WR, Albrektsen G, Royset ES, Gilde B, Sandvik AK, Martinsen TC, Fossmark R. 2019. Mucosal 5-aminosalicylic acid concentration, drug formulation and mucosal microbiome in patients with quiescent ulcerative colitis. Aliment Pharmacol Ther 49:1301–1313. https://doi.org/10.1111/apt.15227.
60. Zhang S, Fu J, Dogan B, Scherl EJ, Simpson KW. 2018. 5-Aminosalicylic acid downregulates the growth and virulence of Escherichia coli associated with IBD and colorectal cancer, and upregulates host anti-inflammatory activity. J Antibiot (Tokyo) 71:950–961. https://doi.org/10.1038/s41429-018-0081-8.
61. Kruis W, Fric P, Pokrotnieks J, Lukas M, Fixa B, Kascak M, Kamm MA, Weismueller J, Beglinger C, Stolte M, Wolff C, Schulze J. 2004. Maintaining remission of ulcerative colitis with the probiotic Escherichia coli Nissle 1917 is as effective as with standard mesalazine. Gut 53:1617–1623. https://doi.org/10.1136/gut.2003.037747.
62. Joeres-Nguyen-Xuan TH, Boehm SK, Joeres L, Schulze J, Kruis W. 2010. Survival of the probiotic Escherichia coli Nissle 1917 (EcN) in the gastrointestinal tract given in combination with oral mesalamine to healthy volunteers. Inflamm Bowel Dis 16:256–262. https://doi.org/10.1002/ibd.21042.
63. Saavedra JT, Schwartzman JA, Gilmore MS. 2017. Mapping transposon insertions in bacterial genomes by arbitrarily primed PCR. Curr Protoc Mol Biol 118:15.15.1–15.15.15.
64. Mulvey MA, Schilling JD, Hultgren SJ. 2001. Establishment of a persistent Escherichia coli reservoir during the acute phase of a bladder infection. Infect Immun 69:4572–4579. https://doi.org/10.1128/IAI.69.7.4572-4579.2001.
65. Rhee KJ, Cheng H, Harris A, Morin C, Kaper JB, Hecht G. 2011. Determination of spatial and temporal colonization of enteropathogenic E. coli and enterohemorrhagic E. coli in mice using bioluminescent in vivo imaging. Gut Microbes 2:34–41. https://doi.org/10.4161/gmic.2.1.14882.